

The Impact of Bed Temperature on Heat Transfer Characteristic between Fluidized Bed and Vertical Rifled Tubes

Artur Blaszcuk^{1*}, Wojciech Nowak²

1. Czestochowa University of Technology, Institute of Advanced Energy Technologies Dabrowskiego 73, 42-200 Czestochowa, Poland
 2. AGH University Science and Technology, Faculty of Energy and Fuels Czarnowiejska 30, 30-059 Cracow, Poland

In the present work, the heat transfer study focuses on assessment of the impact of bed temperature on the local heat transfer characteristic between a fluidized bed and vertical rifled tubes (38mm-O.D.) in a commercial circulating fluidized bed (CFB) boiler. Heat transfer behavior in a 1296t/h supercritical CFB furnace has been analyzed for Geldart B particle with Sauter mean diameter of 0.219 and 0.246mm. The heat transfer experiments were conducted for the active heat transfer surface in the form of membrane tube with a longitudinal fin at the tube crest under the normal operating conditions of CFB boiler. A heat transfer analysis of CFB boiler with detailed consideration of the bed-to-wall heat transfer coefficient and the contribution of heat transfer mechanisms inside furnace chamber were investigated using mechanistic heat transfer model based on cluster renewal approach. The predicted values of heat transfer coefficient are compared with empirical correlation for CFB units in large-scale.

Keywords: Cluster renewal approach, heat transfer coefficient, bed temperature, suspension density, circulating fluidized bed

Introduction

The issue of heat transfer process between the fluidized bed and the boiler surface in the form of water membrane wall plays a critical role in the case of circulating fluidized bed reactors used for the heat recovery and the clean or high efficiency combustion of fossil fuels. Particular attention has been recently drawn to the reduction of the energy intensity of the energy generation process, while meeting the environmental protection requirements laid down by the IED Directive of the European Parliament and the Council [1]. Understanding the complex gas-solid flow pattern and heat transfer processes occurring during solid fuel combustion under circulating fluidized-bed conditions constitutes a factor decisive to the quality of the final product obtained. This applies to the method of receiving and supplying heat to

the heat exchangers, while taking into account the location and geometry of the heatable surfaces. Understanding the mechanisms of heat flow, being in a close correlation with the prevailing hydrodynamic conditions, will provide the necessary knowledge of the process scaling and the design of heat exchange surfaces. The correct sizing of active heat transfer surfaces inside CFB furnace ensures proper operation, load turndown and also affect furnace temperature. The furnace temperature is of importance for the formation and reduction of harmful matter, which influences the economic indices of commercial CFB boilers.

The aims of the current work were to: (i) experimental investigation of bed temperature and suspension density profiles in a 1296t/h supercritical CFB boiler; (ii) present

Nomenclature

a	coefficient in Eq. (2), -	U_{mf}	minimum fluidization velocity, m/s
b	coefficient in Eq. (2), -	U_t	terminal velocity of bed particles, m/s
CFB	circulating fluidized bed, -	Q	boiler load, %

c	coefficient in Eq. (2), -	Y	fraction of particles in the dispersed phase, -
c_g	specific heat of gas, $\text{kJ}/(\text{kg}\cdot\text{K})$	Z	height above air distributor, m
c_p	specific heat of bed particle, $\text{kJ}/(\text{kg}\cdot\text{K})$	Δz	distance between pressure taps, m
D_h	hydraulic diameter, m		
d_p	mean bed particle size, mm		
e	emissivity, -		
f	fractional of wall covered by clusters, -		
G_{sh}	lateral solid circulation flux, $\text{kg}/(\text{m}^2\cdot\text{s})$		
g	acceleration due to gravity, m/s^2		
H	furnace height, m		
h	bed-to-wall heat transfer coefficient, $\text{W}/(\text{m}^2\cdot\text{K})$		
h_c	cluster heat transfer coefficient, $\text{W}/(\text{m}^2\cdot\text{K})$		
h_g	gas convection heat transfer coefficient, $\text{W}/(\text{m}^2\cdot\text{K})$		
h_p	particle convection heat transfer coefficient, $\text{W}/(\text{m}^2\cdot\text{K})$		
h_w	wall contact heat transfer coefficient, $\text{W}/(\text{m}^2\cdot\text{K})$		
k	thermal conductivity, $\text{W}/(\text{m}\cdot\text{K})$		
L_c	cluster characteristic travel length, m		
MCR	maximum continuous rating, -		
p	pressure, kPa		
Δp	pressure drop, kPa		
Pr	Prandtl number, -		
T	temperature, K		
t_c	cluster residence time, s		
U_c	cluster descent velocity, m/s		
U_g	superficial gas velocity, m/s		
		Greek letters	
		δ	wall layer thickness, m
		δ_f	fin depth, mm
		δ_g	gas gap thickness, m
		ε	cross-sectional bed average voidage, -
		μ	viscosity, $\text{kg}/(\text{m}\cdot\text{s})$
		ρ	density, kg/m^3
		ρ_b	suspension density, kg/m^3
		σ	Stefan Boltzmann's constant, $\text{W}/(\text{m}^2\cdot\text{K}^4)$
		Superscripts	
		ad	air dried basis
		ar	as received
		Subscripts	
		b	bed
		c	cluster phase
		cr	radiation from cluster phase
		dr	radiation from dispersed phase
		g	gas
		max	maximum value
		p	particle
		w	wall
		∞	core

overall heat transfer coefficient distributions; and (iii) depict the contribution of heat transfer mechanisms inside furnace as a function of bed temperature.

In summary, this work addresses an existing gap in the literature data regarding the modelling of and experimentation of heat transfer to tubes in furnace chamber [2-6], by providing experimental data from CFB unit in a large-scale. The high labour intensity and cost of carrying out large commercial-scale tests are the cause of the lack of publications of the results of investigations of heat transfer processes on a large commercial scale [7-10]. In this situation, carrying out comprehensive studies would make it possible to establish the optimal heat transfer conditions in correlation with the bed hydrodynamics.

Heat Transfer Process In CFB Furnace

Heat transfer between the fluidized bed and containing walls involves three modes: (i) convection by particles, (ii) convection by gas, (iii) radiation from clusters, and also (iv) radiation from dispersed phase. Contribution of individual heat transfer mechanisms are considered sep-

arately due to the complexity of the bed hydrodynamics. Mechanistic models based on cluster renewal approach commonly assume that the walls are not covered by a continuous stream of solids. In the case of CFB boilers each portion of the active heat transfer surface (i.e. water membrane wall) is intermittently washed by down-flowing clusters of bed particles and dispersed medium. Thus, one part of the heat transfer surface is in contact with cluster while the rest is in contact with the gas or dispersed phase. This fact is due to a major feature of core-annulus flow structure inside CFB furnace as indicated by Fig. 1.

So, the bed-to-wall heat transfer coefficient can be stated in the following equation (1) as the sum of heat transfer mechanisms contributions [12-14]:

$$h = fh_p + (1 - f)h_g + fh_{rc} + (1 - f)h_{rd}, \quad (1)$$

where the subscripts p , g , rc and rd denote particle convection, gas convection, radiation from clusters and radiation from dispersed phase, respectively. In equation (1), the parameter f represents the fractional wall coverage by clusters and is estimated using the hydraulic diameter and height of the CFB furnace in a non-dimen-

sional form:

$$f = 1 - \exp[-a(1-\varepsilon)^b(D_h/H)^c]. \quad (2)$$

To derive values of the coefficient a , b , c in equation (2) heat transfer data from four CFB boilers in large-scale with a different equivalent diameter 1.6 m (12MW_{th}), 5.2 m (20MW_e), 6.2 m (145MW_{th}), 10.6 m (170MW_e) and also at different elevations above the secondary air supply: 11.5 m, 25.0 m, 26.0 m and 30 m were analyzed and then the coefficients have been estimated using multiple regression analysis [9].

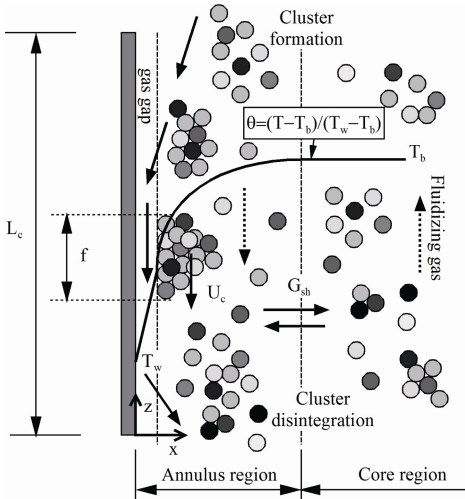


Fig. 1 Single cluster formation and gas gap in the vicinity of the water membrane wall inside CFB furnace [11].

In the cluster renewal model of heat transfer for CFB boilers, particle convection heat transfer coefficient comprises unsteady heat conduction into clusters h_c and the conduction across the thin gas layer between the cluster and the heat transfer surface h_w . Finally, the particle convection heat transfer coefficient h_p is given by:

$$h_p = \left(\frac{1}{h_c} + \frac{1}{h_w} \right)^{-1} = \left(\sqrt{\frac{\pi T_c}{4k_c \rho_c c_c}} + \frac{d_p \delta_g}{k_g} \right)^{-1}. \quad (3)$$

Formulas needed to estimate the physical and thermal properties for the clusters and gas have been detailed described by Blaszczuk et al. [12] and will not be repeated in this work.

When the vertical heat transfer surfaces (i.e. membrane walls) exposes to fluidized bed at large Archimedes number or dilute lean phase, the gas convection component in overall heat transfer coefficient may be expressed as follows [15]:

$$h_g = \frac{k_g c_p}{d_p c_g} \left(\frac{\rho_d}{\rho_p} \right)^{0.3} \left(\frac{U_t^2}{g d_p} \right)^{0.21} \text{Pr}, \quad (4)$$

where k_g denotes thermal conductivity of the gas, d_p represents mean bed particle size, U_t means terminal ve-

locity of the bed particles, c_g and c_p are specific heat of gas phase and particle, respectively. In the above equation (4), g is acceleration due to gravity, ρ_p represents particle density and ρ_d denotes dispersed phase density. In the current heat transfer study, dispersed phase density is found by the following equation:

$$\rho_d = \rho_p Y + \rho_g (1 - Y). \quad (5)$$

In this correlation, Y is the volumetric concentration of bed particles in the dispersed phase and the value of this parameter is recommended as 0.001% [16]. In the heat transfer model, the dispersed phase contains a small concentration of bed particles (i.e. dilute gas-particle mixture) and gas.

The radiation heat transfer from the cluster to the water membrane wall is similar to that between two infinite parallel plates with a view factor 1. Thus, the cluster radiation component of the bed-to-wall heat transfer coefficient is calculated from the expression:

$$h_{rc} = \frac{\sigma (T_c^4 - T_w^4)}{(T_c - T_w) (e_c^{-1} + e_w^{-1} - 1)}, \quad (6)$$

where σ is the Stefan-Boltzmann constant, T_w represents active heat transfer surface temperature, T_c means cluster temperature which is estimated from the empirical correlation for radial temperature distribution proposed by Golriz [17]. In above equation (6), e_c and e_w are the emissivities of the cluster and wall, respectively. The membrane wall emissivity e_w is assumed to have a constant value 0.8, as for oxidized steel. For analysis of heat transfer in commercial CFB combustors, the cluster emissivity can be derived by equation (7) which takes account of bed particle radiation:

$$e_c = 0.5(1 + e_p). \quad (7)$$

Here e_p denotes particle emissivity and is equal to 0.7 as suggested Basu [18]. Thus, the cluster emissivity is larger than particle emissivity.

At high furnace temperature (>973 K) and also region with low suspension density (<5 kg/m³) inside furnace chamber of CFB boilers [18-20], the dispersed radiation component of the overall heat transfer coefficient becomes important and is estimated using the following equation:

$$h_{rd} = \frac{\sigma (T_b^4 - T_w^4)}{(T_b - T_w) (e_d^{-1} + e_w^{-1} - 1)}, \quad (8)$$

where T_b denotes bed temperature, e_d is the emissivity of dispersed phase which may be calculated by the Brewster's relationship for isotropic scattering [21]. The expression for e_d is given as:

$$e_d = \sqrt{\frac{e_p}{(1 - e_p)B} \left(\frac{e_p}{(1 - e_p)B + 2} \right)} - \frac{e_p}{(1 - e_p)B}, \quad (9)$$

For isotropic scattering, B can be taken to equal about 0.5. Other denotations in equation (8) are explained in

equation (6).

Performance Tests and Experimental Conditions

The heat transfer experiments were performed in a 1296 t/h supercritical CFB boiler located in Tauron Generation S.A. Lagisza Power Plant, Poland. More information about the CFB facility can be found in the works [12, 13, 22, 23], in which particularly is presented construction data, cross-sectional area, arrangement of measuring points and also data acquisition system.

The planning of large commercial-scale experiments required a series of preliminary tests to be performed, which involving the observations of the variability of process parameter change rate. Based on these observations, the frequency of process data archiving in accordance with the Shannon-Kotelnikov theorem [24] and the duration of an individual test were selected.

To assessment of the impact of bed temperature on the local heat transfer characteristic between a fluidized bed and vertical rifled tubes, experiments were conducted during a four-day period.

Each test lasted eight hours at four different boiler loads (i.e. 40%MCR, 60%MCR, 80%MCR and 100%MCR). The eight hours for each test were needed in order to establish the repeatability of experimental results. The measurement of furnace data (i.e. static pressure and bed/wall temperature data) was carried out under stable operating conditions. During performance tests on the supercritical CFB boiler with capacity 966MW_{th}, the mass flow of feeding materials supplied into furnace chamber (i.e. coal and limestone) was kept on constant level.

Air fossil fuel firing conditions of performance tests are summarized in Table 1.

For the performance tests described in this paper, bed temperatures between 1063 K and 1183 K were achieved by burning Polish bituminous coal (Ziemowit coal mine, Poland) with approximately 20% excess air. The characteristic of fossil fuel used in the performance tests are given in Table 2.

Determination of proximate parameters of the bituminous coal was made in accordance with applicable standards for fossil fuel in Poland. Meanwhile, the ultimate analysis data were obtained by means of the LECO TrueSpec™ analyzer. All analytical data for fossil fuel are averages from five repetitions for each fuel constituent.

Table 1 Operation parameters of performance tests

Parameter	Unit	Overall range
Boiler loads, Q	%MCR	40–100
Superficial gas velocity, U_o	m/s	3.89–5.11
Minimum fluidization velocity, U_{mf}	m/s	0.0164–0.0243
Voidage at minimum fluidization velocity, ε_{mf}	-	0.40–0.41

Solids circulation rate, G_s	kg/(m ² s)	21.4–25.5
Sauter mean particle diameter, d_{32}	mm	0.219–0.246
Suspension density, ρ_b	kg/m ³	1.55–6.14
Bed temperature, T_b	K	1063–1183
Wall temperature, T_w	K	636–735
Pressure drop, Δp	kPa	6.86–8.25

Table 2 Properties of bituminous coal used in the tests

Ultimate analysis (air dried basis)	Unit	Overall range
C ^{ad} , carbon	wt.%	52.32–56.50
H ^{ad} , hydrogen	wt.%	4.02–4.74
O ^{ad} , oxygen	wt.%	5.35–6.98
N ^{ad} , nitrogen	wt.%	0.73–0.84
S ^{ad} , sulphur	wt.%	0.87–1.21
Proximate analysis (as-received)		
Q ^{ar} , Caloric value	MJ/kg	20.11–22.79
V ^{ar} , Volatile matter	wt.%	25.61–30.37
A ^{ar} , Ash	wt.%	9.10–20.11
M ^{ar} , moisture	wt.%	11.81–19.13

In supercritical CFB boiler above the secondary air injection level (transport zone) are located the active heat transfer surfaces i.e. membrane wall, wing wall evaporators and also radiant super heater. In the current study is considered heat transfer at membrane wall inside furnace chamber. The membrane wall is the main absorbing heat transfer surface from products of solid fuel combustion process. The membrane walls are constructed in the form the membrane rifled tubes with a longitudinal fin at the tube crest. The vertical rifled tubes have a 38mm outside diameter with spacing of 63mm. More detailed information on geometry of membrane walls can be found in the following publications [14, 25].

Results and Discussion

Experimental data used in this heat transfer study are given in dimensionless scale by reason of confidential informations about industrial CFB boilers in large-scale. Besides, suspension density was normalized by maximum value obtained during all tests.

In this heat transfer study, the concept of mechanistic heat transfer model is used to investigate the heat transfer mechanism behavior near the vertical rifled tubes, according to the cluster renewal approach. The bed-to-wall heat transfer coefficient and contribution of heat transfer components along furnace chamber are generated based on the experimental conditions given in Table 1.

Bed-to-wall heat transfer coefficient distribution along furnace height at different bed temperature for a 1296 t/h

supercritical CFB boiler is depicted in Fig. 2.

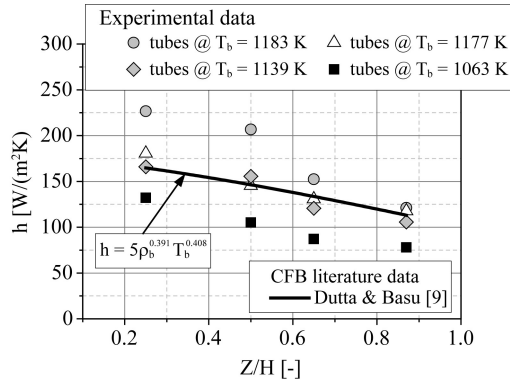


Fig. 2 Bed-to-wall heat transfer coefficient variation with furnace height of CFB boiler at different bed temperature.

With increase in bed temperature, heat transfer coefficient increases for the same non-dimensional distance Z/H from the air distributor level. The bed-to-wall heat transfer coefficient increases with bed temperature for higher fractional of wall covered by clusters. This fact is due to the combined effect of increased cluster heat transfer and reduced gas gap resistance due to higher gas thermal conductivity. Other reason for the higher bed-to-wall heat transfer coefficient arises from suspension density variations along furnace height of CFB boiler.

Figure 3 illustrates a strong influence of suspension density on the bed-to-wall heat transfer coefficient.

In our heat transfer study, solid suspension density was calculated by the following empirical correlation:

$$\rho_b = -\frac{1}{g} \frac{\Delta p}{\Delta z}, \quad (10)$$

where Δp represent pressure drop and Δz denotes distance between pressure taps. Attrition and gas-particle acceleration effects were neglected in equation (10).

The bed temperature has an essential effect on the heat transfer data at high relative suspension density. In the case of low normalized suspension density, the bed temperature has negligible impact of the overall heat transfer coefficient. In addition, it can be seen from Fig. 3 that the influence of solid suspension density diminishes with bed temperature. In Fig. 3, the heat transfer data obtained using the cluster renewal approach were correlated by the non-linear function using the regression analysis. The heat transfer grey curves in Fig. 3 have steeper slope in the experimental data region. In addition, it can be seen from Fig. 3 that there is not much difference between the experimental data points for the cluster renewal approach and the published experimental data for Chalmers and Dalhousie boiler [9, 26] at the suspension density varied in the range of 2–4 kg/m³. In the case of suspension den-

sity covering the range of 5.44–6.14 kg/m³ was observed significant difference.

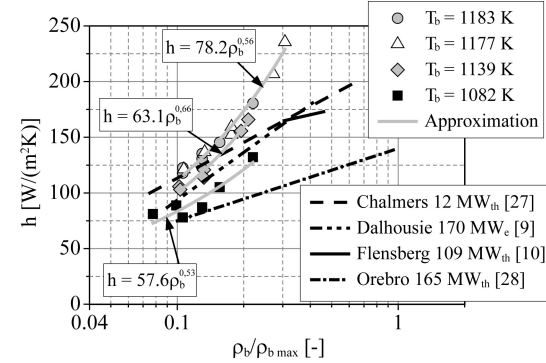


Fig. 3 Bed-to-wall heat transfer coefficient distribution as a function of the bed temperature and the normalized suspension density.

Figures 4–7 illustrate contribution of heat transfer mechanisms at different bed temperature inside CFB furnace. Contribution of heat transfer mechanisms is drawn as individual colour and type line for each heat transfer mode. In this heat transfer study, the gas convection contribution was not significant in the bed-to-wall heat transfer coefficient, as demonstrated by Figs 4–7.

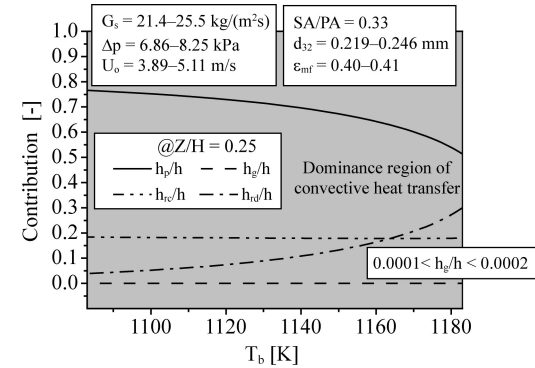


Fig. 4 Contribution of heat transfer mechanisms as a function of bed temperature at $Z/H=0.25$

At non-dimensional height coordinate Z/H of 0.25 (lower region of transport zone) was recognized high bed particles concentration and more clusters in comparison with other elevations above the fluidization grid (i.e. $0.5 < Z/H < 0.87$). Due to high suspension density in the vicinity of the vertical rifled tubes, particle convection component in heat transfer mechanisms prevails in the overall heat transfer coefficient. The high particle convection heat transfer results from the thermal conductivity of cluster. The cluster thermal conductivity increases with bed temperature due to higher gas thermal conductivity. The resistance due to gas gap thickness between cluster and rifled tubes was reduced due to increased gas thermal conductivity. The value of

h_{rd}/h increases with the increase of bed temperature. The experimental tests show that radiation from cluster phase not depend upon furnace temperature direct above the slope section of furnace chamber.

At the half CFB furnace height ($Z/H=0.5$), radiative heat transfer plays dominant role in heat transfer mechanisms whereas bed temperature exceed 1125 K. This fact indicates significant role of suspension density and also furnace temperature (i.e. wall and bed temperature) on contribution of heat transfer modes between the fluidized bed and the active heat transfer surface inside CFB furnace. The slope of particle convection curve is directly proportional to bed particle concentration and bed temperature. The same trend was also confirmed by [12]. The radiation from clusters slowly decreases with the increase of radiation from dispersed phase.

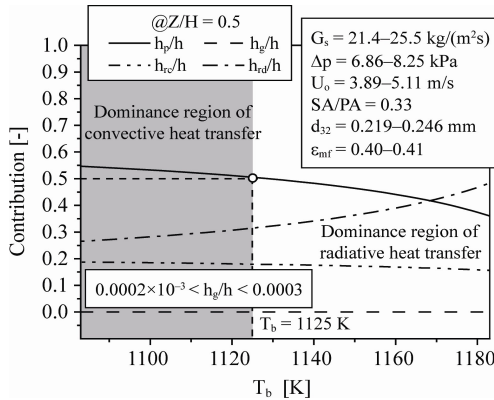


Fig. 5 Contribution of heat transfer mechanisms as a function of bed temperature at $Z/H=0.5$

The variations of heat transfer mechanisms contribution in the exit region of furnace chamber occupied by membrane wall and radiant superheater SH II (transport zone at $0.65 < Z/H < 0.87$) are presented in Figs. 6–7.

The shape of profiles for h_p/h , h_r/h and also h_{rd}/h contribution is almost the same, both for $Z/H=0.65$ and $Z/H=0.87$. The upper part of furnace chamber was operated in a dilute phase ($\rho_b < 1.55 \text{ kg/m}^3$) whereas the middle and lower regions of transport zone were a dense phase ($\rho_b > 6 \text{ kg/m}^3$). As can be seen in Figs. 6–7, dilute phase radiation heat transfer h_{rd} increases with bed temperature and is characterized by a linear function for non-dimensional distance $0.65 < Z/H < 0.87$. Nevertheless, the radiation from dispersed phase at $0.25 < Z/H < 0.5$ is characterized by exponential function. This conclusion is consistent with the results presented in Figs. 4–5. Moreover, a similar trend of the heat transfer components variation was observed by Basu [18], when CFB unit was operated at 70% load condition. Due to sufficient low suspension density (dilute phase) and high bed temperature in the exit region of furnace chamber, radiation from dispersed phase has dominant role in heat

transfer mechanisms from core region to vertical rifled tubes.

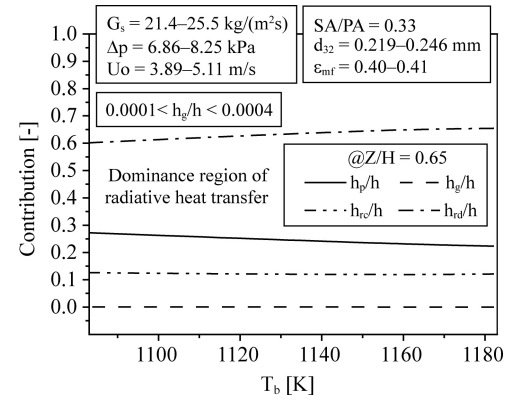


Fig. 6 Contribution of heat transfer mechanisms as a function of bed temperature at $Z/H=0.65$

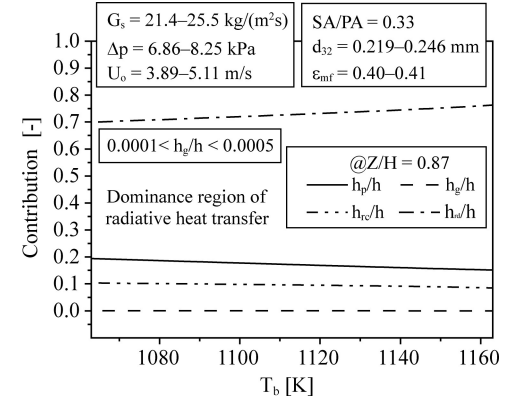


Fig. 7 Contribution of heat transfer mechanisms as a function of bed temperature at $Z/H=0.87$

The performance tests show that there is interplay of bed particle concentration and clusters in contributions of particle convection and radiation from clusters. Under dilute phase conditions the active heat transfer surface was covered by less clusters (ca. $f=13\%$) than in a dense region of transport zone (ca. $f=68\%$).

Conclusions

In this heat transfer study, the mechanistic heat transfer model with integrates bed hydrodynamics in CFB furnace was used to assessment of the effect of bed temperature on heat transfer behavior in CFB coal combustor. A heat transfer analysis was carried out between fluidized bed and vertical rifled tubes based on cluster renewal approach. Heat transfer data were compared with published literature data for CFB units in large-scale. The experimental data agree quite well with the results for CFB boilers in large-scale. The experimental measurements of furnace data (bed temperature and suspension

density) show that bed-to-wall heat transfer coefficient was strongly correlated with furnace height. The bed temperature and suspension density affected the overall heat transfer coefficient. This conclusion was also confirmed by authors [18, 19, 28]. Obtained heat transfer data prove the effect of fraction of wall exposed to clusters on particle heat transfer coefficient, especially at non-dimensional distance of 0.25 and also 0.5 from fluidization grid. The low particle concentration (suspension density) and low value of the parameter f contribute to decrease of convection heat transfer mechanism. Meanwhile, the radiation from dispersed phase proportion increased with increase in bed temperature. In the upper part of combustion chamber occupied by superheater SH, the contribution of the radiative heat transfer coefficient was dominant in the bed-to-wall heat transfer. This is due to sufficient high bed temperature and also low suspension density. The contribution of radiation from clusters does not exceed 20% and 12% for $0.25 < Z/H < 0.5$ and $Z/H > 0.65$ respectively. The gas convection heat transfer mechanism was negligible during all performance tests. The heat transfer data will be useful in the design and scale-up of heat exchangers operated in circulating fluidized bed conditions. Very important and useful for the development of computation methods and the design of commercial CFB boilers is the comprehensive study of the impact of bed temperature on the heat transfer mechanisms behavior. The observed variation of heat transfer mode will give fundamental design basic for fluidized bed systems

Acknowledgments

The authors would like to gratefully acknowledge the staff of Tauron Generation S.A. Lagisza Power Plant for technical support with supplying operating data and construction data. The authors like to express sincere thanks to Szymon Jagodzik: Lagisza Power Plant, Poland for kindly making the manuscript more readable. This work was financially supported by scientific research No BS-PB-406/301/11.

References

- [1] Directive 2010/75/EU of the European Parliament and the Council on industrial emissions (integrated pollution prevention and control) adopted on 24 November 2010.
- [2] Ludowski, P., Taler, D., Taler J., 2013, Identification of thermal boundary conditions in heat exchangers of fluidized bed boilers, *Appl. Therm. Eng.*, 58, pp. 194–204.
- [3] Taler, J., Duda, P., Węglowski, B., Zima, W., Grądzik, S., Sobota, T., Taler, D., 2009, Identification of local heat flux to membrane water-walls in steam boilers, *Fuel*, 88, pp. 305–311.
- [4] Taler, J., Taler, D., Ludowski, P., 2014, Measurements of local heat flux to membrane water walls of combustion chambers, *Fuel*, 115, pp. 70–83.
- [5] Zima, W., Grądzik, S., Cebula, A., 2010, Modeling of heat and flow phenomena occurring in water wall tubes of boilers for supercritical steam parameters, *Arch. Thermodyn.*, 31, pp. 19–36.
- [6] Lu, Y., Zhang, T., Dong, X., 2015, Bed to wall heat transfer in supercritical water fluidized bed: Comparision with the gas-solid fluidized bed, *Appl. Therm. Eng.*, 88, pp. 297–305.
- [7] Cheng, L., Wang, Q., Shi, Z., Luo, Z., Ni, M., Cen, K., 2007, Heat transfer in a large-scale circulating fluidized bed boiler, *Front. Energy Power Eng.*, 1, pp. 477–482.
- [8] Andersson, B., Leckner, B., 1992, Experimental methods of estimating heat transfer in circulating fluidized bed boilers, *Int. J. Heat Mass Tran.*, 35, pp. 3353–3362.
- [9] Dutta, A., Basu, P., 2005, An improved cluster-renewal model for the estimation of heat transfer coefficients on the furnace walls of commercial circulating fluidized bed boilers, *J. Heat Trans. - T ASME*, 126, 1040–1043.
- [10] Wedermann, C.C., Werther, J., 1994, Heat transfer in large-scale circulating fluidized bed combustors of different sizes, in: Avidan A. (Ed.), *Circulating Fluidized Bed Technology IV*, American Institute of Chemical Engineers, New York, pp. 428–435.
- [11] Blaszcuk, A., Nowak, W., 2014, Bed-to-wall heat transfer coefficient in a supercritical CFB boiler at different bed particle sizes, *Int. J. Heat Mass Tran.*, 79, pp. 736–749.
- [12] Blaszcuk, A., Nowak, W., 2015, Heat transfer behavior inside a furnace chamber of large-scale supercritical CFB reactor, *Int. J. Heat Mass Tran.*, 87, pp. 464–480.
- [13] Blaszcuk, A., Nowak, W., Jagodzik, Sz., 2014, Bed-to-wall heat transfer in a supercritical circulating fluidized bed boiler, *Chem. Process Eng.*, 35, pp. 191–204.
- [14] Blaszcuk, A., 2015, Effect of flue gas recirculation on heat transfer in a supercritical circulating fluidized bed combustor, *Arch. Therm.*, 36, pp. 61–83.
- [15] Basu, P., Cheng, L., Cen, K. 1996, Heat transfer in a pressurized circulating fluidized bed, *Int. J. Heat Mass Trans.*, 39, pp. 2711–2722.
- [16] Basu, P., Fraser, S.A., 1991, *Circulating Fluidized Bed Boilers-Design and Operation*, Butterworth-Heinemann, Stoneham.
- [17] Grace, J.R., 1982, Fluidized bed heat transfer, in: G. Hestrone (Ed.), *Handbook of Multiphase Flow*, McGraw-Hill, Hemisphere, Washington, DC.
- [18] Basu, P., 2006, *Combustion and Gasification in Fluidized Beds*, CRC Press.
- [19] Kunii, D., Levenspiel, O., 1991, *Fluidization Engineering*,

2nd edition, Butterworth-Heinemann, Stoneham.

[20] Bucak, O., Dogan, O.M., Uysal, B.Z., 1999, Heat transfer in circulating fluidized bed combustor, in: R.B. Reuther (Ed.), *Proceedings of 15th International Conference on Fluidized Bed Combustion*, ASME, Savannah, Georgia, USA.

[21] Brewster, M.Q., 1986, Effective absorptivity and emissivity of particulate media with application to fluidized bed, *Trans. ASME J. Heat Transfer*, 108, pp. 710–713.

[22] Blaszcuk, A., Leszczynski, J., Nowak, W., 2013, Simulation model of mass balance in a supercritical circulating fluidized bed combustor, *Powder Technol.*, 246, pp. 317–326.

[23] Blaszcuk, A., Zylka, A., Leszczynski, J., 2015, Simulation of mass balance behavior in a large-scale circulating fluidized bed reactor, *Particuology*, DOI: 10.1016/j.partic.2015.04.003 (in press).

[24] Marks, R.J., 2009, *Handbook of Fourier Analysis & Its Applications*, Oxford University Press, New York.

[25] Blaszcuk, A., Nowak, Jagodzik, Sz., 2014, The impact of bed particle size in heat transfer to membrane walls of supercritical CFB boiler, *Arch. Therm.*, 35, pp. 207–223.

[26] Andersson, B., Leckner, B., 1992, Experimental methods of estimating heat transfer in circulating fluidized bed boilers, *In. J. Heat Mass Tran.*, 35, pp. 3353–3362.

[27] Divilio, R.J., Boyd, T.J., 1994, Practical implication of the effect of solids suspension density on heat transfer in large-scale CFB boilers, in: Avidan A. (Ed.), *Circulating Fluidized Bed Technology IV*, American Institute of Chemical Engineers, New York, pp. 334–339.

[28] Reddy, B.V., 2002, Fundamental heat transfer mechanism between bed-to-membrane water-walls in circulating fluidized bed combustors, *Int. J. Energy Res.*, 27, pp. 813–824.